

# Effect of the phase on the dynamics of a perturbed bouncing ball system

Sijo K. Joseph\*, Inés P. Mariño, Miguel A.F. Sanjuán

*Nonlinear Dynamics, Chaos and Complex Systems Group, Departamento de Física, Universidad Rey Juan Carlos, Tulipán s/n, 28933 Móstoles, Madrid, Spain*

## ARTICLE INFO

### Article history:

Received 14 September 2011

Received in revised form 15 December 2011

Accepted 15 December 2011

Available online 27 December 2011

### Keywords:

Control of chaos

Phase control of chaotic systems

Bouncing ball map

Intermittency and crisis

## ABSTRACT

The phase control method is a non-feedback control technique which has been used for different purposes in continuous periodically driven dynamical systems. One of the main goals of this paper is to apply this control technique to the bouncing ball system, which can be seen as a paradigmatic periodically driven discrete dynamical system, and has a rather simple physical interpretation. The main idea is to apply a periodic control signal including a phase difference with respect to the periodic forcing of the initial system and to analyze its effect on the dynamics of the bouncing ball system. The numerical simulations we have carried out clearly show the strong effect of the phase of the control signal in suppressing or generating chaotic behavior and in changing the period of a periodic orbit. We have also analyzed the effect of the phase in the phenomenon of the crisis-induced intermittency, showing how the phase enhances the size of the attractor near a crisis and can induce the intermittent behavior. Finally we have analyzed the scaling behavior of the crisis by varying the phase difference between the perturbation and the external forcing.

© 2011 Elsevier B.V. All rights reserved.

## 1. Introduction

In 1949, Fermi [1] proposed an acceleration mechanism of cosmic ray particles interacting with the time-dependent magnetic field. Later on Stanislaw Ulam explained this phenomenon in terms of a simple classical model in which a ball is bouncing between two heavy harmonically oscillating walls [2]. This model became popular as the Fermi–Ulam model [3] and several modified versions were proposed over the years because of its interesting dynamical properties [4,5]. Among the different models, the simplest one that displays chaotic behavior is the system with one ball bouncing on a vibrating table under the action of gravity. This is widely known as the bouncing ball system [6,7]. It is a discrete dynamical system, since the time evolution of the dynamics of the system is discontinuous at collisions.

Chaos control methods might be classified into two categories, depending on how they interact with the chaotic system. The first category corresponds to feedback methods, which are aimed to stabilize one of the stable orbits that lie in the chaotic attractor by applying small perturbations that depend on the time-varying state of the system. However, the fast response to the time variations of the system state makes its experimental implementation difficult. For this reason, non-feedback methods have appeared more useful in many practical cases. They allow to switch between different dynamical behaviors by applying either parameter perturbations or external forcing signals that do not depend on the current state of the system [8–10].

We are focusing here on a non-feedback control method, the phase control method, which has been hardly explored and applied to discrete dynamical systems. In this method the phase of the applied perturbation is used to change the dynamical system behavior. Moreover implementing experimentally this non-feedback method is rather easy. This technique has been

\* Corresponding author.

E-mail address: [sijo.joseph@urjc.es](mailto:sijo.joseph@urjc.es) (S.K. Joseph).

used so far to control different dynamical properties of continuous dynamical systems [11–16]. Similar ideas have been also applied in the context of Josephson junctions [17] and in population dynamics in Theoretical Ecology [18].

In a simple bouncing ball model, the ball is bouncing on a sinusoidally vibrating table under the action of gravity. If the impact between the table and the ball is inelastic, we can represent the velocity of the ball just after the impact with the help of a discrete map which is called the bouncing ball map [6,7]

$$\begin{aligned}x_{n+1} &= x_n + y_n, \\y_{n+1} &= \alpha y_n + \beta \cos(x_n + y_n).\end{aligned}\tag{1}$$

Here the variable  $x_n$  is the time interval between the  $(n - 1)$ th and the  $n$ th collisions of the ball and  $y_n$  is the velocity of the ball immediately after the  $n$ th impact. The parameter  $\alpha \in (0, 1]$  is the coefficient of restitution and the parameter  $\beta$  is associated with the table frequency. If the coefficient of restitution is  $\alpha = 1$  then Eq. (1) reduces to the standard map.

The paper is organized as follows. Section 2 is devoted to explaining the phase control method and to show how it can be applied on the bouncing ball map. In this way, we set the ground for different applications of this technique, which are addressed in the remaining sections. In particular, in Section 3 we analyze the effect of the phase of the perturbation to suppress the chaotic behavior in the bouncing ball system and to create and annihilate periodic windows. The effect of the phase of the perturbation on intermittencies and crises is investigated in Section 4. Finally, conclusions are given in Section 5.

## 2. Phase control method

Non-feedback methods have been mainly used to suppress chaos in periodically driven dynamical systems of the form

$$\dot{\mathbf{x}} = \mathbf{f}(\mathbf{x}, \mathbf{p}) + \mathbf{F} \cos(\omega t),\tag{2}$$

where  $\mathbf{x}$  and  $\mathbf{F}$  are  $m$ -dimensional vectors and  $\mathbf{f} : \mathbb{R}^m \times \mathbb{R}^n \rightarrow \mathbb{R}^m$ , being  $n$  the dimension of the parameter vector  $\mathbf{p}$  and  $\omega$  the frequency of the external forcing.

The main idea of these non-feedback methods is to apply a harmonic perturbation to one of the parameters of the periodically driven system

$$\dot{\mathbf{x}} = \mathbf{f}(\mathbf{x}, p_1, \dots, p_{i-1}, p_i(1 + \epsilon \cos(r\omega t + \phi)), p_{i+1}, \dots, p_n) + \mathbf{F} \cos(\omega t)\tag{3}$$

or as an external perturbation to the periodically driven system,

$$\dot{\mathbf{x}} = \mathbf{f}(\mathbf{x}, \mathbf{p}) + \mathbf{F} \cos(\omega t) + \epsilon \mathbf{u} \cos(r\omega t + \phi),\tag{4}$$

where  $\mathbf{u}$  is a conveniently chosen unitary vector, the parameter  $r$ , termed resonance condition, determines the ratio between the frequency of the perturbation and the frequency of the external forcing, and  $\phi$  is the phase difference between the perturbation and the external forcing.

In parametric perturbation methods [10,19], the numerical and experimental explorations have been essentially focused on the role of the perturbation amplitude  $\epsilon$  and the resonance condition  $r$ , but the role of the phase difference  $\phi$  has hardly been explored. However, we claim that the latter parameter  $\phi$  has a relevant influence on the dynamical behavior of the system that demands further study. For this reason we apply the phase control technique to the bouncing ball system of Eq. (1), by adding a harmonic perturbation to the parameter  $\beta$ . This is equivalent to adding an external perturbation on the table oscillation of amplitude  $\epsilon\beta$ . As a consequence, we obtain the following map,

$$\begin{aligned}x_{n+1} &= x_n + y_n, \\y_{n+1} &= \alpha y_n + \beta(1 + \epsilon \sin(2\pi r n + \phi)) \cos(x_n + y_n),\end{aligned}\tag{5}$$

where  $\epsilon$ ,  $\phi$  and  $r$  are free parameters, and  $\alpha = 0.1$  is fixed throughout our calculations. When the forcing amplitude  $\epsilon$  is zero, this map reduces to the simple bouncing ball map. One of the key elements of this control method is to assume that the amplitude of the external perturbation is very small, therefore, fixing  $r$  and keeping  $\epsilon$  small enough, we can use  $\phi$  as the only free parameter to control the system [11–13].

Experimental realization of this control method is relatively simple since we need to change only the phase of the control signal. On the perturbed nonlinear map the perturbation is applied to  $\beta$ . The parameter  $\beta$  is related to the amplitude and the square of the frequency of the table vibration. If we slightly modulate the table amplitude and change the phase of the modulation we can achieve control in the system. We can also do the same by modulating the frequency of the table vibration and changing the phase. The third option is adding a small external perturbation to the table as an additional driving force and by changing the phase of the external force we can control the system.

## 3. Controlling the dynamics of the bouncing ball system

Now we are going to consider the effect of the phase on the dynamical system behavior. In particular, we analyze here the use of the phase control method to suppress the chaotic behavior and the creation and annihilation of periodic windows in the bouncing ball system.

In order to analyze the effect of the phase control on the bouncing ball system, first we have to observe the dynamics of the system without control. Let us consider the bifurcation diagram of the unperturbed system, obtained by changing the value of the parameter  $\beta$ , shown in Fig. 1. We can see regions of chaotic behavior together with some periodic windows. For example, the one centered at  $\beta = 6$  and the one centered at  $\beta = 10.3$  (see the arrows in Fig. 1).

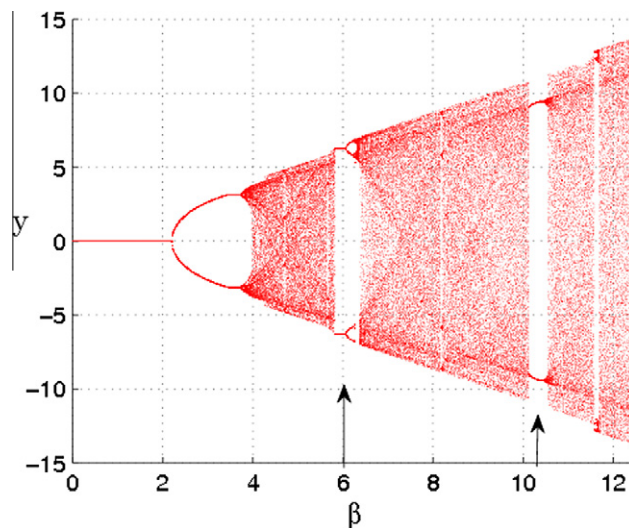
By tuning the phase of the periodic perturbation it is possible to change the behavior of the system from chaotic to periodic and vice versa. In order to evaluate in a detailed way the role of  $\epsilon$  and  $\phi$ , we calculate the largest Lyapunov exponent  $\lambda$  over every point in a  $200 \times 200$  grid. These points belong to the rectangle  $0.02 \leq \epsilon \leq 0.07$ ,  $0 \leq \phi \leq 2\pi$ . The results for  $r = 0.5$ , 1.0, 1.5, 2.0 are plotted in Fig. 2(a)–(d), respectively, where we have considered  $\beta = 6.56$ . The black and white colors associated to each point in the  $(\epsilon, \phi)$  plane indicate the negative and positive sign of the largest Lyapunov exponent, respectively. If it is positive the dynamics is chaotic and if it is negative the system shows periodic behavior.

Fig. 2 shows that there exist wide regions of the  $(\epsilon, \phi)$  plane where the largest Lyapunov exponent  $\lambda$  is negative, and therefore chaos is suppressed. We note that the black region of periodic behavior (with negative Lyapunov exponent), far from having a trivial or irregular shape, presents a symmetry that depends on the parity of the parameter  $r$ . When  $r$  is an odd multiple of 0.5, we can observe that the region of periodic behavior (black) is symmetric around  $\phi = \pi$ . When  $r$  is an even multiple of 0.5, the black region is symmetric around  $\phi = 2\pi$  (note that the range of the phase in the plots is only  $0 \leq \phi \leq 2\pi$ ). The most interesting feature is the role of the phase  $\phi$  in selecting the final state of the system. We have plotted the bifurcation diagram (Fig. 3) by setting  $\alpha = 0.1$ ,  $r = 0.5$ ,  $\epsilon = 0.03$  and  $\phi = \pi/2$  which is inside the black region of Fig. 2(a). One of the main results is that it is possible to avoid chaos with a suitable choice of the phase of the perturbation  $\phi$ .

Another interesting phenomenon in Fig. 3 is the appearance and the disappearance of periodic windows. If we compare the bifurcation diagram when the perturbation is not applied (Fig. 1) with the one when the perturbation is applied (Fig. 3), we can see that a new periodic window arises under perturbation when  $\beta = 4$ . At the same time we can observe that the periodic window centered at  $\beta = 10.3$  vanishes. This method is particularly useful both to generate and to suppress chaos in a dynamical system.

A way to explain the mechanism behind the creation and annihilation of periodic windows is through the Melnikov analysis, by which we can calculate the Melnikov distance [20]. The Melnikov distance gives the distance between the stable and the unstable manifolds of the perturbed systems measured along the direction perpendicular to the unperturbed homoclinic orbit. If  $\Delta(t)$  denotes the Melnikov distance, then  $\Delta(t) = \epsilon(M(t, \alpha, \beta, \phi) + O(\epsilon))$ , where the function  $M(t, \alpha, \beta, \phi)$  is the Melnikov integral which depends on the system parameters including the phase value  $\phi$ . A zero of the function  $M(t, \alpha, \beta, \phi)$  denotes a homoclinic point, hence it shows a Smale–Birkhoff horseshoe type of chaos [20]. Since  $M(t, \alpha, \beta, \phi)$  depends on the phase value, the zeroes of the function can be adjusted by tuning the parameter  $\phi$ . Thus, by tuning the phase of the perturbation, we can generate chaos as well as suppress it.

We have also found through numerical simulations that, by a proper choice of the phase  $\phi$  it is possible to change the period of a periodic orbit. As an example, we can consider the bouncing ball map with  $\alpha = 0.1$  and  $\beta = 6.0$  and take  $x_0 = 0$ ,  $y_0 = 1$  as the initial condition. For this parameter values and initial condition the system exhibits an orbit of period one. If the phase control method is applied the period of the orbit can be increased. In particular, taking  $\epsilon = 0.03$  and  $r = 0.5$ , for  $\phi = 0.3$  the system exhibits an orbit of period two, for  $\phi = \pi/4$  the system exhibits an orbit of period four, and for  $\phi = \pi/2$  it exhibits an orbit of period eight. It is also interesting to note that the basin of attraction of a periodic orbit can be modified as the phase  $\phi$  is increased.



**Fig. 1.** Bifurcation diagram of the bouncing ball system as a function of the parameter  $\beta$ . We can observe here two wide periodic windows at  $\beta = 6$  and at  $\beta = 10.3$ .

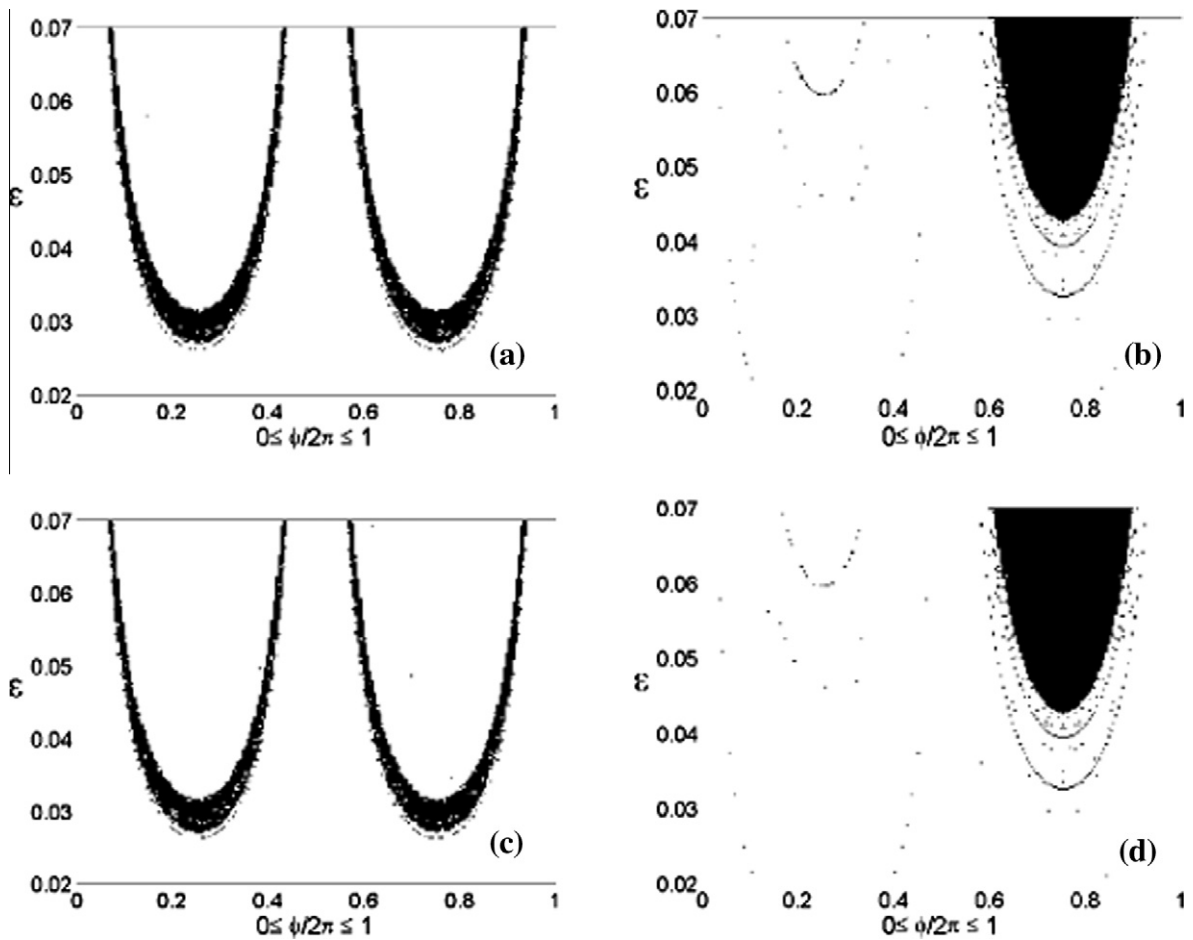


**Fig. 2.** The figure shows the sign of the largest Lyapunov exponent  $\lambda$  computed at every point of a  $200 \times 200$  grid of  $(\epsilon, \phi)$  values. The range of variation is  $0 \leq \phi \leq 2\pi$ ,  $0.02 \leq \epsilon \leq 0.07$  for different values of the resonant condition, (a)  $r = 0.5$ , (b)  $r = 1.0$ , (c)  $r = 1.5$  and (d)  $r = 2.0$ . The Lyapunov exponent is negative in the black regions. These regions have a structure that follows the expected symmetry around  $\phi = \pi$  when  $r$  is an odd multiple of 0.5 and the trivial symmetry around  $\phi = 2\pi$  for an even multiple of 0.5. We set the parameters  $\beta = 6.56$ ,  $\alpha = 0.1$ .

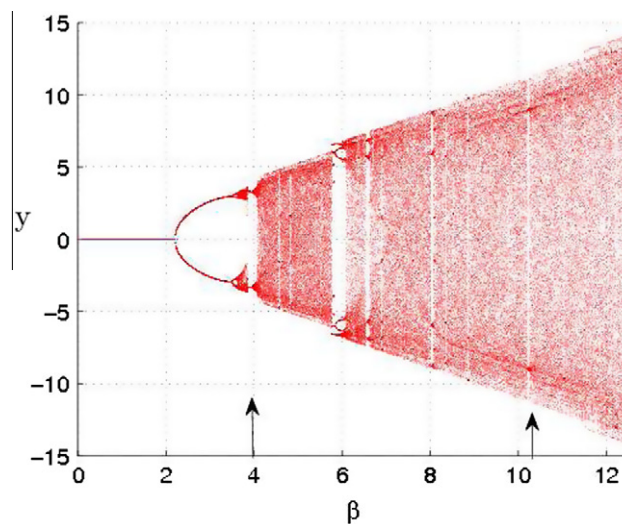


**Fig. 3.** Bifurcation diagram of the bouncing ball system when the control is applied. On the  $y$ -axis we have the velocity of the bouncing ball. We see that a new periodic window arises under perturbation when  $\beta = 4$ , at the same time the periodic window centered at  $\beta = 10.3$  disappears. Here the perturbation parameters are taken as  $\alpha = 0.1$ ,  $r = 0.5$ ,  $\epsilon = 0.03$  and  $\phi = \pi/2$ .

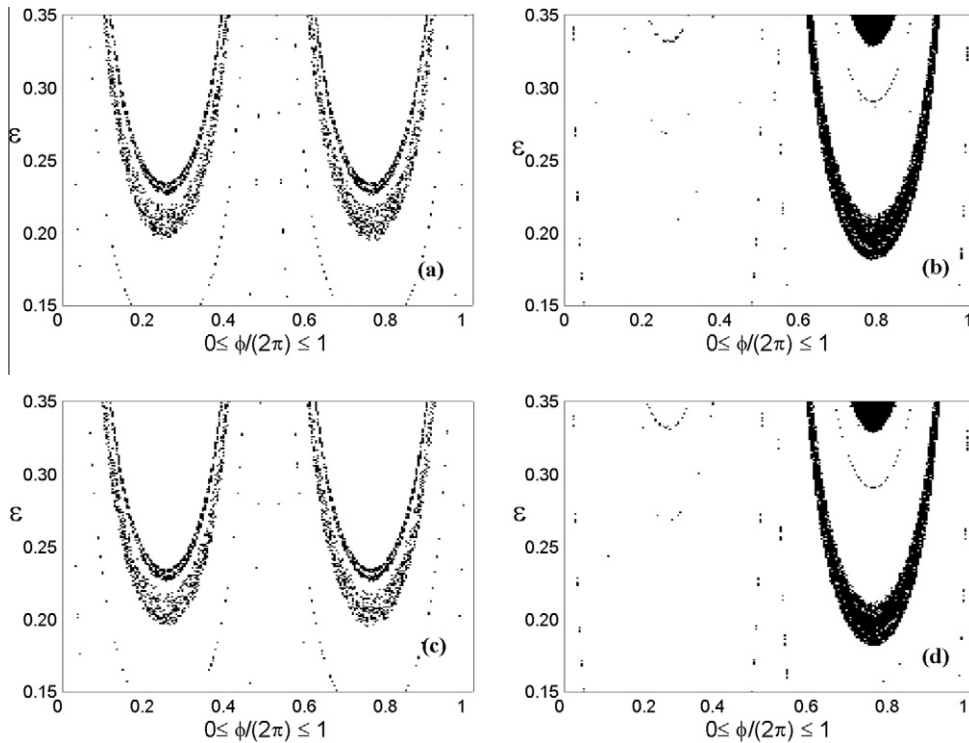


**Fig. 4.** The figure shows the sign of the largest Lyapunov exponent  $\lambda$  computed at every point of a  $200 \times 200$  grid of  $(\epsilon, \phi)$  values for a different value of the coefficient of restitution  $\alpha = 0.3$  and taking the same value of  $\beta = 6.56$  used in Fig. 2. The range of variation is  $0 \leq \phi \leq 2\pi$ ,  $0.15 \leq \epsilon \leq 0.35$  for different values of frequency ratio, (a)  $r = 0.5$ , (b)  $r = 1.0$ , (c)  $r = 1.5$  and (d)  $r = 2.0$  respectively. The largest Lyapunov exponent is negative in the black regions. We observe that the width of this region remains almost the same but we need higher values of  $\epsilon$  to control chaos in the system.

Fig. 4 shows the sign of the largest Lyapunov exponent  $\lambda$  computed at every point of a  $200 \times 200$  grid of  $(\epsilon, \phi)$  values for a different value of the coefficient of restitution  $\alpha = 0.3$ . Fig. 4(a)–(d) corresponds to  $r = 0.5$ ,  $r = 1.0$ ,  $r = 1.5$ ,  $r = 2.0$  respectively. In all these plots we observe that the width of the control region where the largest Lyapunov exponent is negative remains basically the same. The main difference is that we need higher values of  $\epsilon$  to control chaos in the system. This is due to the fact that the dissipation in the system decreases as the parameter  $\alpha$  is increased. Hence we have to spend more energy to control the system.

#### 4. Phase dependent intermittency and crisis

By modifying a control parameter, a chaotic attractor can touch an unstable periodic orbit inside its basin of attraction inducing a sudden expansion. This phenomenon is called interior crisis. Beyond the crisis the system preserves a memory of the former situation, so a fraction of the time is spent in the region corresponding to the pre-crisis attractor, and during the rest of the time; excursions around the formerly unstable periodic orbit take place. This behavior is known as crisis-induced intermittency [21]. Before the crisis, such excursions cannot take place unless a noise or an external perturbation induces them. In this paper, we show that the intermittency at an interior crisis can be controlled by using the phase control technique. We give numerical evidence that an appropriate value of the phase  $\phi$  can be used to enhance the size of the attractor near the crisis and induce the corresponding intermittent behavior. An experimental and theoretical study of the phase control of intermittency in a laser system was carried out by Zambrano et al. [13].

Here we are interested in a discrete dynamical system. First of all we need a good indicator to determine the size of the attractor for different values of the corresponding parameters. This indicator has been chosen as

$$\langle H \rangle = \langle \max(y_n) \rangle, \tag{6}$$

that represents the average value of the relative maxima of the time series  $y_n$  (recall that  $y_n$  is the velocity of the bouncing ball right after the  $n$ th impact).

Fig. 5 represents the value of  $\langle H \rangle$  computed at every point of a  $200 \times 200$  grid of  $(\epsilon, \phi)$  values in the region  $0 \leq \phi \leq 2\pi$ ,  $0.02 \leq \epsilon \leq 0.07$  for the perturbed bouncing ball map when considering  $\beta = 4.05$  and  $r = 0.5$ . The wide symmetrical white regions in Fig. 5 show that there is an expansion in the attractor. Notice that, once fixed the value of  $\epsilon$ , only for some specific values of the phase  $\phi$  there exists such expansion in the attractor, which in turn leads to intermittency. From Fig. 5 we can

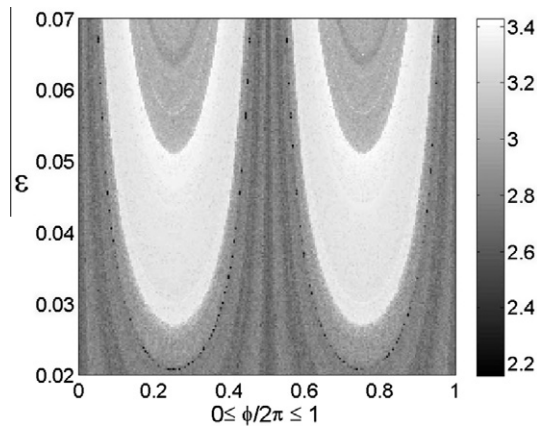


**Fig. 5.** Average value of the relative maxima of the velocity,  $\langle H \rangle$ , computed at every point of a  $200 \times 200$  grid of  $(\epsilon, \phi)$  values in the region  $0 \leq \phi \leq 2\pi$ ,  $0.02 \leq \epsilon \leq 0.07$  for the perturbed bouncing ball map. The white region shows the sudden expansion in the attractor. Here we set the parameters  $\alpha = 0.1$ ,  $\beta = 4.05$  and  $r = 0.5$ .

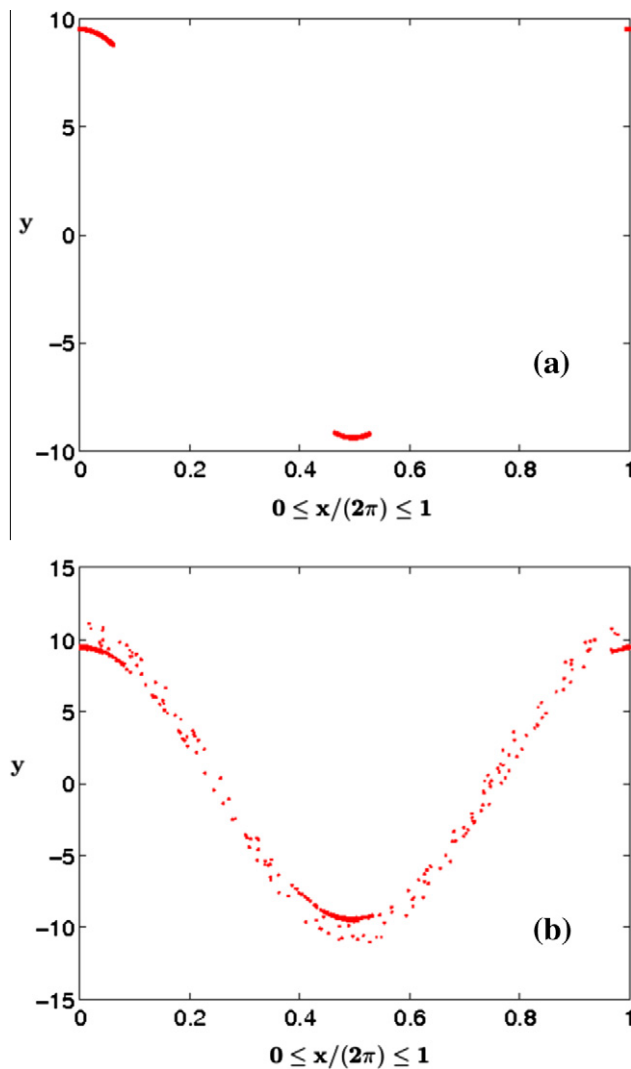


**Fig. 6.** (a) The figure shows the chaotic three-piece attractor just before ( $\phi = 0.27650$ ) the interior crisis. (b) The figure shows the enlarged attractor just after the interior crisis ( $\phi = 0.27660$ ). The system has an interior crisis at  $\phi_c \approx 0.27655$ . The dense points in the enlarged attractor gives the attractor in the pre-crisis regime and the enlarged dotted region gives the intermittency. The parameter values are set to  $\alpha = 0.1$ ,  $\beta = 10.4$ ,  $r = 0.5$  and  $\epsilon = 0.03$ .

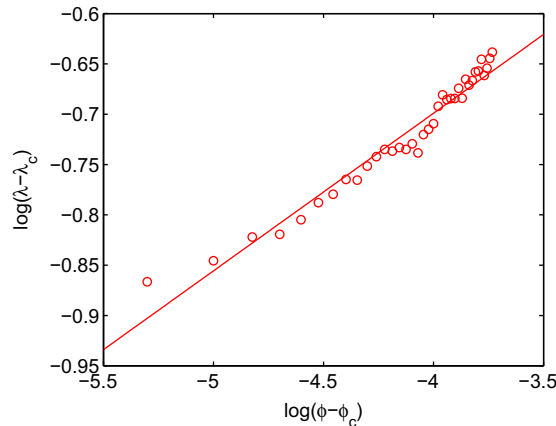


**Fig. 7.** Graph of  $\log(\lambda - \lambda_c)$  versus  $\log(\phi - \phi_c)$ . The slope of the linear best fit yields the value of the scaling exponent  $\gamma = 0.15$  with a norm of residuals 0.07. Here we vary  $\phi$  from 0.276615 to 0.276800 with an increment of  $5 \times 10^{-6}$ .

also observe a symmetry in the phase value of the applied signal which induces the internal crisis in the system. This can be explained in terms of the symmetry of the map under the transformation  $\phi \rightarrow \phi + \pi$  for this particular value of  $r$ .

In order to gain a deeper insight into the role of the phase  $\phi$  in nonlinear systems we study the perturbed map close to an interior crisis. Fig. 6(a) shows the phase space of the perturbed bouncing ball map when  $\phi = 0.27650$  and Fig. 6(b) shows the phase space of the perturbed bouncing ball map when  $\phi = 0.27660$ . In both cases we set  $\alpha = 0.1$ ,  $\beta = 10.4$ ,  $r = 0.5$  and  $\epsilon = 0.03$ . We can see a three-piece chaotic attractor just before the crisis in Fig. 6(b) and observe in Fig. 6(a) the sudden expansion of the attractor when the phase value is increased by a small amount. We can also observe in Fig. 6(b) that the enlarged attractor consists of the attractor in the pre-crisis regime and the enlarged dotted region that gives the intermittency. The dotted region represents the leaking trajectories from one piece of the attractor to another. Here, a change in the phase enhances the size of the attractor, which in turn induces the intermittency.

We have also analyzed the scaling property of the phase close to the critical point after the occurrence of the crisis. Notice that in the post-crisis regime the dynamics describing the evolution of the system is intermittent. The average time a chaotic orbit spends in the region of the pre-crisis attractor  $\langle \tau \rangle$ , as the control parameter  $\phi$  is varied, obeys a scaling law which was proposed by Grebogi et al. [21]. It is found that  $\langle \tau \rangle \sim |\phi - \phi_c|^{-\gamma}$  where  $\gamma$  is the scaling exponent and  $\phi_c$  denotes the critical value of the phase at which the crisis happens. The behavior of the Lyapunov exponents near the crisis point for the dissipative standard map was studied by Pompe and Leven [22]. According to them, the increase of the largest Lyapunov exponent near the crisis is a consequence of the rapid growth of the transition probability. Thus, we can say that the average time a chaotic orbit spends in the region  $\langle \tau \rangle$  is inversely proportional to the Lyapunov exponents. In other words, the size of the attractor is related to the Lyapunov exponent via the Kaplan–Yorke dimension. Thus the new scaling equation reads

$$\lambda(\phi) - \lambda(\phi_c) \sim |\phi - \phi_c|^\gamma, \quad (7)$$

where  $\lambda(\phi)$  denotes the largest Lyapunov exponent at the corresponding value of the phase. Crises with such kind of scaling behavior result from the collision of the chaotic attractor with the stable manifold of an unstable periodic orbit.

The scaling law for the characteristic times of noise induced crises is studied by Sommerer et al. [23]. According to them, the noise induced crises result from the noise kicking a trajectory across the gap between the attractor and the unstable fixed point or its pre-image. In the phase control method a deterministic sinusoidal perturbation is playing the role of the noise. When we are tuning the phase, we are adjusting the kick strength acting on the trajectory. Hence by selecting an appropriate value of the phase we can enhance the size of the attractor in the system.

We have numerically assessed the validity of the scaling law of the average of the largest Lyapunov exponent versus the phase of the applied signal near the crisis regime. The behavior of the Lyapunov exponent near the crisis regime has been studied by several authors [24,25]. We have calculated the average of the largest Lyapunov exponent using  $10^2$  initial conditions over an orbit length of  $10^4$  iterations as shown in Fig. 7 and varied the phase  $\phi$  from 0.276615 to 0.276800 with an increment of  $5 \times 10^{-6}$ . The slope of the linear best fit gives the value of the scaling exponent  $\gamma = 0.15$  with the norm of residuals 0.07.

## 5. Conclusions

We have successfully applied the phase control method, that had been applied in continuous periodically driven dynamical systems, to the bouncing ball map. This map can be considered as a paradigmatic periodically driven discrete dynamical system, and since its models the bouncing ball system, it is rather easy to have a physical intuition about the meaning of the

variation of the parameters. So, the main idea has been to implement the control technique into this well-known map and to analyze the effect of the phase on the dynamics of the bouncing ball system. One of the first results obtained is to observe the strong effect of the phase of the control signal in suppressing or generating chaotic behavior. Another aspect that we have analyzed is the effect of the phase in inducing the intermittent behavior near a crisis. The phase actually may help to enhance the size of the attractor and contribute to the crisis-induced intermittency phenomenon. Finally, we have analyzed the scaling behavior of the crisis by varying the phase difference between the perturbation and the external forcing.

## Acknowledgement

This work was supported by the Spanish Ministry of Science and Innovation under Project No. FIS2009–09898.

## References

- [1] Fermi E. On the origin of the cosmic radiation. *Phys Rev* 1949;75:1169–74.
- [2] Ulam S. On some statistical properties of dynamical systems. In: Neyman J, Oxtoby JC, editors. *Proceedings of the fourth Berkeley symposium on mathematical statistics and probability*, vol. 3. Berkeley: University of California Press; 1961. p. 315–20.
- [3] Lieberman MA, Lichtenberg AJ. Stochastic and adiabatic behavior of particles accelerated by periodic forces. *Phys Rev A* 1971;5:1852–66.
- [4] Leonel ED, McClintock PVE. Effect of a frictional force on the Fermi–Ulam model. *J Phys A: Math Gen* 2006;39:11399.
- [5] Brahic A. Numerical study of a simple dynamical system. I. The associated plane area-preserving mapping. *Astron Astrophys* 1971;12:98–110.
- [6] Holmes PJ. The dynamics of repeated impacts with a sinusoidally vibrating table. *J Sound Vib* 1982;84:173–89.
- [7] Guckenheimer J, Holmes PJ. *Nonlinear oscillations, dynamical systems, and bifurcations of vector fields*. Berlin: Springer; 1983.
- [8] Sanjuán MAF. Using nonharmonic forcing to switch the periodicity in nonlinear systems. *Phys Rev E* 1998;58:4377–82.
- [9] Braiman Y, Goldhirsch I. Taming chaotic dynamics with weak periodic perturbations. *Phys Rev Lett* 1991;66:2545–8.
- [10] Hsu RR, Su HT, Chern JL, Chen CC. Conditions to control chaotic dynamics by weak periodic perturbation. *Phys Rev Lett* 1997;78:2936–9.
- [11] Zambrano S, Seoane JM, Mariño IP, Sanjuán MAF, Meucci R. Phase control in nonlinear systems. In: Sanjuán MAF, Grebogi C, editors. *Recent progress in controlling chaos*. Singapore: World Scientific; 2010. p. 147–87.
- [12] Zambrano S, Allaria E, Brugioni S, Leyva I, Meucci R, Sanjuán MAF, et al. Numerical and experimental exploration of phase control of chaos. *Chaos* 2006;16:013111.
- [13] Zambrano S, Mariño IP, Salvadori F, Meucci R, Sanjuán MAF, Arechi FT. Phase control of intermittency in dynamical systems. *Phys Rev E* 2006;74:016202.
- [14] Seoane JM, Zambrano S, Euzzor S, Meucci R, Arechi FT, Sanjuán MAF. Avoiding escapes in open dynamical systems using phase control. *Phys Rev E* 2008;78:016205.
- [15] Zambrano S, Seoane JM, Mariño IP, Sanjuán MAF, Euzzor S, Meucci R, et al. Phase control of excitable systems. *New J Phys* 2008;10:073030.
- [16] Seoane JM, Zambrano S, Mariño IP, Sanjuán MAF. Basin boundary metamorphoses and phase control. *Europhys Lett* 2010;90:30002.
- [17] Chitra RN, Kuriakose VC. Phase effects on synchronization by dynamical relaying in delay-coupled systems. *Chaos* 2008;18:023129; Chitra RN, Kuriakose VC. Phase synchronization in an array of driven Josephson junctions. *Chaos* 2008;18:013125; Chitra RN, Kuriakose VC. Dynamics of coupled Josephson junctions under the influence of applied fields. *Phys Lett A* 2007;365:284–9.
- [18] Greenman JV, Pasour VB. Phase control of resonant systems: interference, chaos and high periodicity. *J Theor Biol* 2011;278:74–86.
- [19] Lima R, Pettini M. Suppression of chaos by resonant parametric perturbations. *Phys Rev A* 1990;41:726–33.
- [20] Glasser ML, Papageorgiou VG, Bountis TC. Mel'nikov's function for two-dimensional mappings. *SIAM J Appl Math* 1989;49:692–703.
- [21] Grebogi C, Ott E, Romeiras F, Yorke JA. Critical exponents for crisis-induced intermittency. *Phys Rev A* 1987;36:5365–80.
- [22] Pompe B, Leven RW. Behaviour of Lyapunov exponents near crisis points in the dissipative standard map. *Phys Scr* 1988;38:651.
- [23] Sommerer JC, Ott E, Grebogi C. Scaling law for characteristic times of noise-induced crises. *Phys Rev A* 1991;43:1754–69.
- [24] Mehra V, Ramaswamy R. Maximal Lyapunov exponent at crises. *Phys Rev E* 1996;53:3420–4.
- [25] Stynes D, Hanan WG, Pouryahya S, Heffernan DM. Scaling relations and critical exponents for two dimensional two parameter maps. *Eur Phys J B* 2010;77:469–78.